# NASA Contractor Report 165664



# Advanced Composite Aileron For L-1011 Transport Aircraft-- Ground Tests And Flight Evaluation

**C.F. Griffin**
Lockheed Corporation
Lockheed-California Company
Post Office Box 551
Burbank, California 91520

**CONTRACT NAS1-15069**
**FEBRUARY 1981**



National Aeronautics and Space Administration
**Langley Research Center**
Hampton Virginia 23665

This Page Intentionally Left Blank

## FOREWORD

This report was prepared by the Lockheed-California Company, Lockheed Corporation, Burbank, California, under contract NAS1-15069. It is the final report of Task IV, ground tests and flight checkout. The program is sponsored by the National Aeronautics and Space Administration (NASA), Langley Research Center. The Program Manager for Lockheed is Mr. F. C. English and the Project Manager for NASA, Langley is Mr. H. L. Bohon. The Technical Representative for NASA, Langley is Dr. H. A. Leybold.

The following Lockheed personnel were principal contributors to the program during Task IV: C. Griffin, Project Engineer; L. Fogg, Structural Analysis; S. Bocarsley and F. Dorward, Testing.

This Page Intentionally Left Blank

TABLE OF CONTENTS


| | | Page |
|---|---|---|
| | FOREWORD | iii |
| | SUMMARY | 1 |
| | INTRODUCTION | 2 |
| | MEASUREMENT VALUES | 3 |
| 1. | DESCRIPTION OF TEST ARTICLES | 4 |
| 1.1 | Aileron General Description | 4 |
| 1.2 | Structural Configuration - Metal Aileron | 4 |
| 1.3 | Structural Configuration - Composite Aileron | 6 |
| 1.4 | Weight and Balance of Test Articles | 8 |
| 2. | STIFFNESS AND VIBRATION TESTS | 9 |
| 2.1 | Stiffness Tests | 9 |
| 2.2 | Vibration Tests | 10 |
| 3. | STATIC TESTS | 12 |
| 3.1 | Test Set-Up and Instrumentation | 12 |
| 3.2 | Test Conditions | 15 |
| 3.3 | Condition 4 Testing | 15 |
| 3.4 | Condition 1 Testing | 18 |
| 4. | DAMAGE TOLERANCE/FAIL-SAFE TESTS | 24 |
| 4.1 | Test Set-Up and Instrumentation | 24 |
| 4.2 | Damage Tolerance Tests | 27 |
| 4.3 | Fail-Safe Tests | 29 |
| 4.4 | Residual Strength Test | 31 |
| 6. | FLIGHT CHECK-OUT | 33 |
| | CONCLUSIONS | 34 |

LIST OF FIGURES


| Figure | | Page |
|---|---|---|
| 1 | Master schedule | 3 |
| 2 | Inboard aileron location on the wing. | 5 |
| 3 | Inboard aileron dimensions. | 5 |
| 4 | Current aluminum aileron. | 6 |
| 5 | Advanced composite aileron assembly | 7 |
| 6 | Torsional stiffness test setup. | 9 |
| 7 | Vibration test set-up | 11 |
| 8 | Loading Installation Arrangement Geometry | 12 |
| 9 | Test set-up for static ground tests | 13 |
| 10 | Aileron cover (upper and lower) - strain gage locations | 13 |
| 11 | Aileron front spar - strain gage locations. | 14 |
| 12 | Aileron main rib at Inboard Aileron Station 102.7 - strain gage locations | 14 |
| 13 | Composite aileron deflection transducer locations | 16 |
| 14 | Condition 4 actuator link reaction loads. | 17 |
| 15 | Condition 4, upper cover strains at I.A.S. 85.7 | 18 |
| 16 | Condition 4, chordwise strains-cover/upper rib cap at I.A.S. 102.7 | 19 |
| 17 | Condition 4, spar cap strains at I.A.S. 97.4 | 19 |
| 18 | Condition 4, I.A.S. 102.7 rib web strains at gage 23 | 20 |
| 19 | Condition 4, I.A.S. 102.7 rib web strains at gage 24 | 20 |
| 20 | Static ground test article with lower cover removed | 21 |
| 21 | Closeup view of I.A.S. 102.7 rib showing web Failure-outboard side | 22 |
| 22 | View of I.A.S. 102.7 rib showing web failure-inboard side | 22 |
| 23 | Closeup view of I.A.S. 107.1 rib showing web Failure-outboard side | 23 |
| 24 | View of I.A.S. 107.1 rib showing web failure-inboard side | 23 |
| 25 | Comparison of design loads to test loads for I.A.S. 102.7 rib. | 25 |

LIST OF FIGURES (Continued)


| Figure | | Page |
|---|---|---|
| 26 | Comparison of stress resultants - test loads Versus design loads | 26 |
| 27 | Upper cover impact damage | 28 |
| 28 | Lower surface impact delamination (front face) | 30 |
| 29 | Lower surface burn-through and impact damage (back face) | 30 |
| 30 | Lower surface swept-stroke damage simulation | 30 |
| 31 | I.A.S. 102.7 rib web failure, residual strength test | 32 |
| 32 | I.A.S. 107.1 rib web failure, residual strength test | 32 |
| 33 | Flight conditions investigated | 33 |

LIST OF TABLES


| Table | | Page |
|---|---|---|
| 1 | Test Article Weight and Inertia Comparisons . . . . . | 8 |
| 2 | Torsional Stiffness Comparisons . . . . . | 10 |
| 3 | Frequency Comparisons . . . . . | 11 |
| 4 | Predicted Aileron Failure Loads . . . . . | 16 |

# ADVANCED COMPOSITE AILERON FOR L-1011 TRANSPORT AIRCRAFT

## GROUND TESTS AND FLIGHT EVALUATION

C. F. Griffin
Lockheed California Company

Summary

The activities documented in this report are associated with Task IV of the Advanced Composite Aileron program. These activities include: comparative stiffness and vibration tests on a metal aileron and on a composite aileron, static tests of a full-scale aileron, damage growth/fail-safe tests on a second full-scale aileron, and flight testing of the composite ailerons.

A composite aileron and a metal aileron were subjected to a series of comparative stiffness and vibration tests to substantiate the flutter integrity of the composite aileron. These tests showed that the stiffness and vibration characteristics of the composite aileron are similar to the metal aileron and meet or exceed the structural requirements.

The first composite ground test article was statically tested to loads greater than design ultimate for two loading conditions. Failure occurred at 139 percent of design ultimate load.

The second composite ground test article was tested to verify the damage tolerance and fail-safe characteristics of the design. Visible damage was inflicted to the aileron at four locations and the damaged aileron was subjected to one lifetime of spectrum fatigue loading. A small amount of damage growth occurred at one location. After conducting limit load tests on the aileron, major damage was inflicted to the cover to simulate damage from swept-stroke lightning. The test article successfully withstood two failsafe loading conditions and was finally loaded to failure. Failure occurred at 130 percent of design ultimate load.

A shipset of composite ailerons was installed on Lockheed's L-1011 flight test aircraft and flown. The composite aileron was flutter-free throughout the flight envelope.

## INTRODUCTION

The broad objective of NASA's Aircraft Energy Efficiency (ACEE) Composite Structures Program is to accelerate the use of composite materials in aircraft structures by developing technology for early introduction of structures made of these materials into commercial transport aircraft. This program, one of several which are collectively aimed toward accomplishing this broad objective, has the specific goal to demonstrate the weight and cost/saving potential of secondary structures constructed of advanced composite materials. The secondary structure selected for the program is the inboard aileron of the Lockheed L-1011 transport aircraft.

The scope of this program is to design, fabricate, qualify, and certificate a composite inboard aileron; to test selected subcomponents to verify the design; to fabricate and test two ground test articles; to fabricate and install five shipsets of inboard composite ailerons; and to gather flight service data on the five shipsets.

The Lockheed-California Company is teamed with Avco Aerostructures Division of Avco Corporation to accomplish program goals. Lockheed designed the aileron, conducted the materials, concept verification, and ground tests, and will evaluate inflight service experience. Avco developed manufacturing processes, fabricated test specimens, and fabricated the ground test and flight articles.

As shown on the master schedule, figure 1, the program is being conducted in six nonsequential tasks. Task I, Engineering Development, and Task II, Design and Analysis, are the portions of the program wherein the composite aileron design was formulated and subcomponents fabricated and tested to verify design concepts and fabrication procedures. During Task III, Manufacturing Development, and Task IV, Ground Test and Flight Checkout, production quality manufacturing tools were constructed, and two full-scale ailerons were fabricated and tested. A production run of five shipsets are

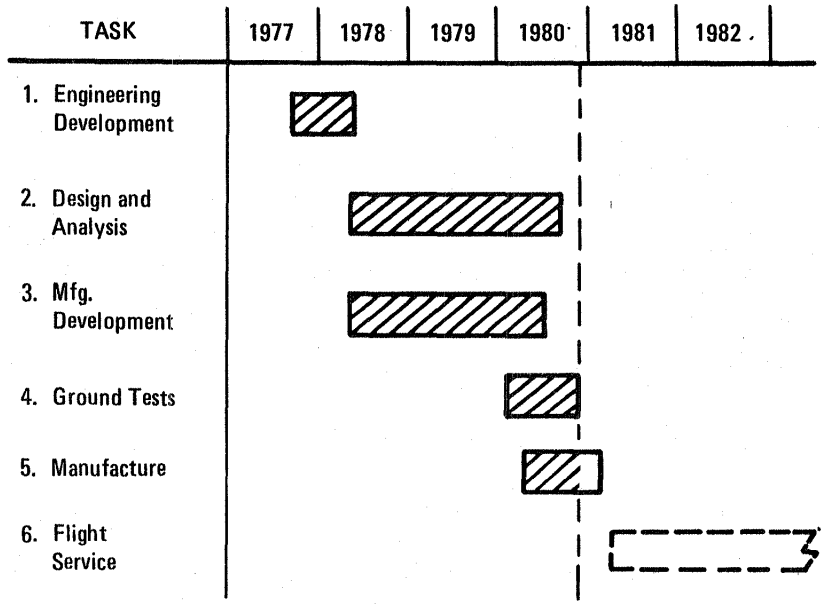


Figure 1. - Master schedule.

being fabricated during Task V, Aileron Manufacture, to provide manufacturing and cost information. In Task VI, Flight Service, inspection and maintenance data will be gathered on the five shipsets to assess their potential for economical operation in routine service. The work performed during this program is intended to provide the data required to progress toward a production commitment.

This report describes work accomplished during Task IV.

## MEASUREMENT VALUES

All measurement values in this technical report are expressed in the International System of Units and customary units. Customary units are used for the principal measurements and calculations.

# 1. DESCRIPTION OF TEST ARTICLES

## 1.1 Aileron General Description

The inboard aileron is located on the wing trailing edge between the outboard and inboard trailing edge flaps and is directly behind the engine, as shown in figure 2. It is supported from the wing at two hinge points and operated by three hydraulic actuators. Basic dimensions of the inboard aileron are shown in figure 3. It is a wedge-shaped, one-cell box beam, thinning slightly from inboard to outboard. The planform is trapezoidal, with parallel leading and trailing edges.

## 1.2 Structural Configuration - Metal Aileron

An illustration of the current aluminum inboard aileron is shown in figure 4. The box consists of a front beam, rear beam, and upper and lower skins, joined by hinge ribs and airload ribs. The front beam consists of a web with access holes and extruded caps. Attached to the web are formers supporting the shroud, which consists of two aluminum clad sheets bonded together.

The rear beam is an I section extrusion with lightening holes in the web. Upper and lower skins are clad aluminum sheets with bonded doublers and are attached to the rib caps with rivets on the upper surface and screws on the lower surface.

Joining the front and rear beams are 18 ribs at about 178 mm (7 in) pitch, most of which are airload ribs. These are of channel extrusion truss construction. The two main actuator ribs are of cap and corrugated web construction, with fittings at the front beam to accommodate hinge and actuator loads, and with titanium straps splicing the upper rib caps and skin to the front beam cap.

The trailing-edge wedge is a sandwich construction and is attached to the rear beam in three discontinuous sections with screws. The end fairings

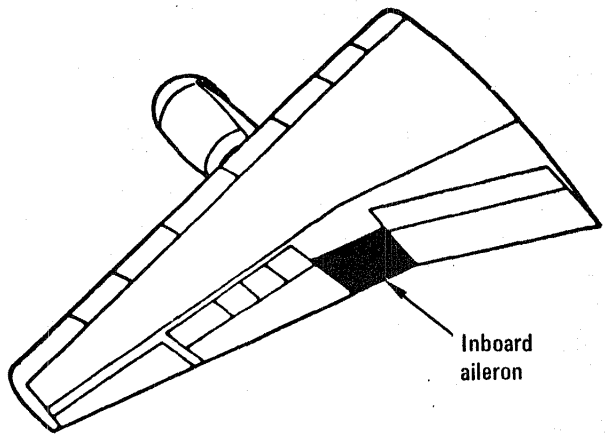


Figure 2. - Inboard aileron location on the wing.

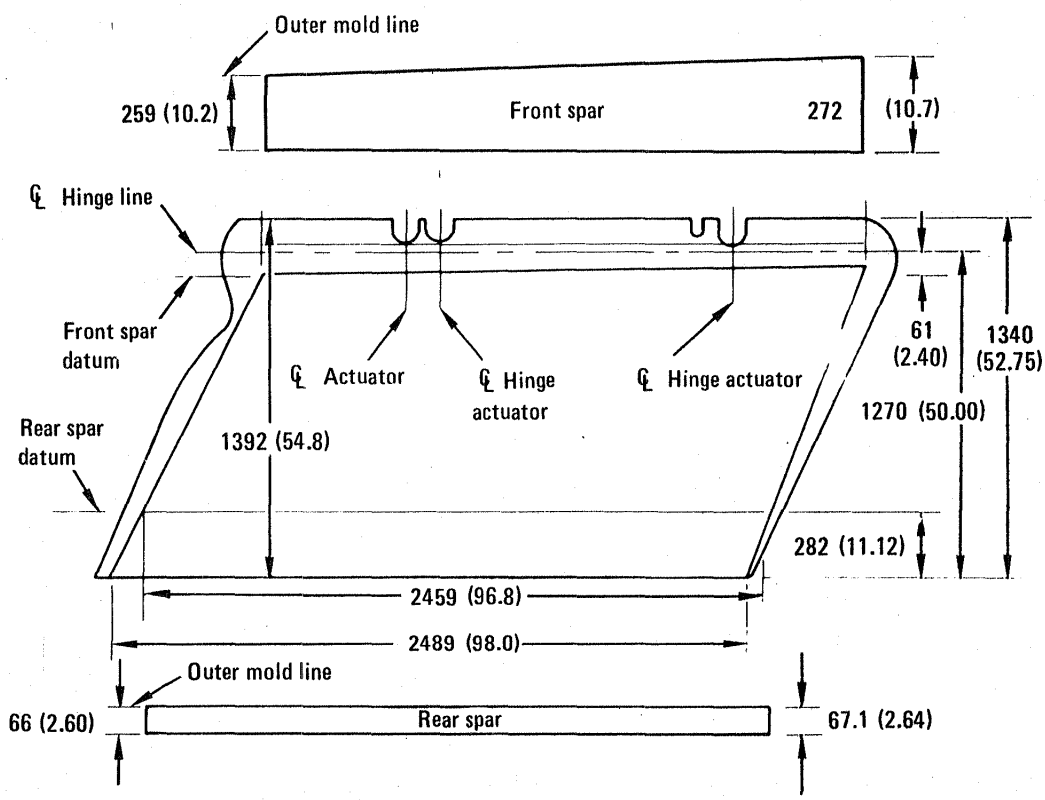


Figure 3. - Inboard aileron dimensions. (All dimensions shown in mm (in))

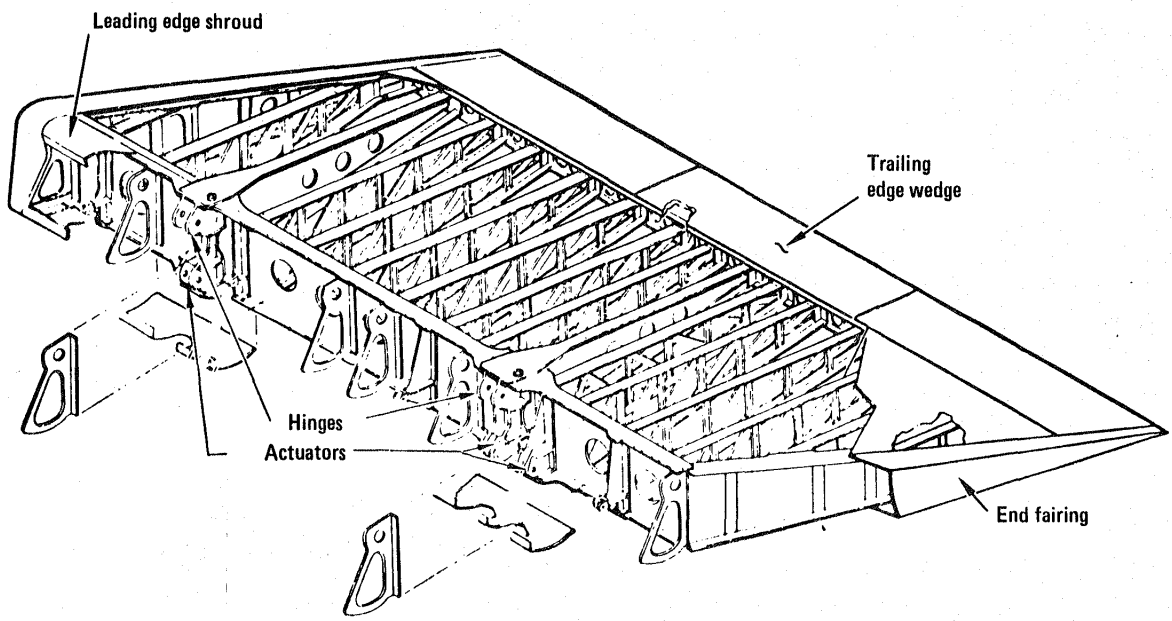


Figure 4. - Current aluminum aileron.

are of beaded fiberglass construction, attached to the close-out rib caps with screws.

The aileron support fittings are aluminum two-piece forgings, joined by Hi-Tigue fasteners. The hinge bearing housings are separate split fittings bolted to the aileron support fittings.

### 1.3 Structural Configuration - Composite Aileron

The selected design for the advanced composite aileron is a multirib configuration with single-piece upper and lower covers mechanically fastened to the substructure. Covers and front spar of the aileron are fabricated with graphite/epoxy unidirectional tape. Graphite/epoxy bidirectional fabric is used for construction of the ribs. The rear spar is fabricated from 7075-T6 clad aluminum alloy sheet. A schematic of the composite aileron assembly is shown on figure 5.

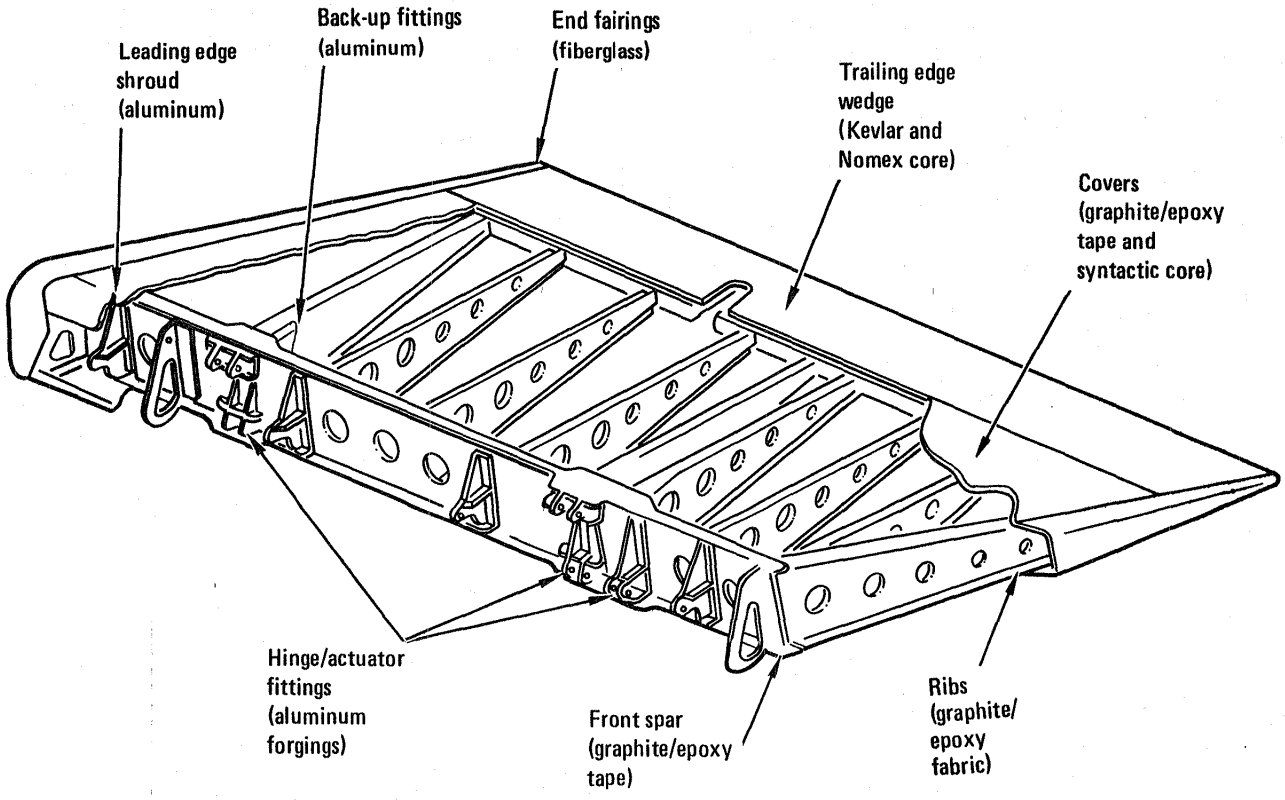


Figure 5. - Advanced composite aileron assembly.

The upper surface, ribs, and spars are permanently fastened with Triwing titanium screws and stainless steel Hi-Lok collars. The removable lower surface, trailing edge wedge, leading edge shroud, and end fairings are attached with the same type of screws but with stainless steel nut plates attached to the substructure with stainless steel cherry rivets.

To preclude galvanic corrosion, aluminum parts are anodized, primed with epoxy and then given a urethane topcoat. Graphite/epoxy parts in contact with aluminum parts are also painted with a urethane topcoat. Faying surface sealant is used at the interface of all aluminum and composite parts. After assembly the aileron is primed and painted. No protection is required against swept-stroke lightning.

Several of the subassemblies that are currently being used on the metal aileron have been incorporated into the composite aileron design. These include the aluminum hinge/actuator fittings, the aluminum leading edge shroud, the Kevlar 49/epoxy trailing edge wedge and the fiberglass/epoxy end fairings.

## 1.4 Weight and Balance of Test Articles

The weight of the test articles was measured by suspending the articles from an electronic load cell. Static unbalance of the test articles was determined by supporting the article on knife edges at the hinge location and measuring the force applied to the trailing edge required to balance the aileron. Determination of the test article mass moment of inertia was accomplished by supporting the aileron on knife edges at the hinge locations with the unbalanced weight supported at the trailing edge by a load transducer placed in series with a tension spring. The aileron was oscillated about the hinge line by imparting a small force to the trailing edge. The period of oscillation was measured with a stop watch and the mass moment of inertia computed.

The weight and balance data for the test articles are displayed in table 1.

TABLE 1. - TEST ARTICLE WEIGHT AND INERTIA COMPARISONS

| | Metal | Composite Article #1 | Composite Article #2 |
|---|---|---|---|
| Weight kg (lb) | 62.6 (138.0) | 49.0 (108.0) | 48.4 (106.8) |
| Static Unbalance N-m (in-lb) | 257 (2272) | 195 (1730) | * |
| Moment of Inertia about Hinge Line N-m$^2$ (lb-in$^2$) | 246 (85700) | 187 (65000) | * |

*Not measured

## 2. STIFFNESS AND VIBRATION TESTS

### 2.1 Stiffness Tests

Comparative tests were conducted on the metal aileron and composite ailerons to determine chordwise bending and torsional stiffness characteristics.

The chordwise stiffness was determined by applying a distributed load to the rear spar of the aileron and reacting the loads at the hinge/actuator fittings. Displacements of the aileron were measured at various positions on the surface and the stiffness computed. Results of these tests indicated that the composite aileron had slightly less chordwise bending stiffness than the metal aileron.

Torsional stiffness characteristics of the ailerons was determined by applying equal and opposite loads at two locations on the rear spar and reacting the loads at the hinge/actuator fittings. Surface deflections were measured to allow computation of the aileron torsional stiffness. A schematic of the test set-up is shown in Figure 6.

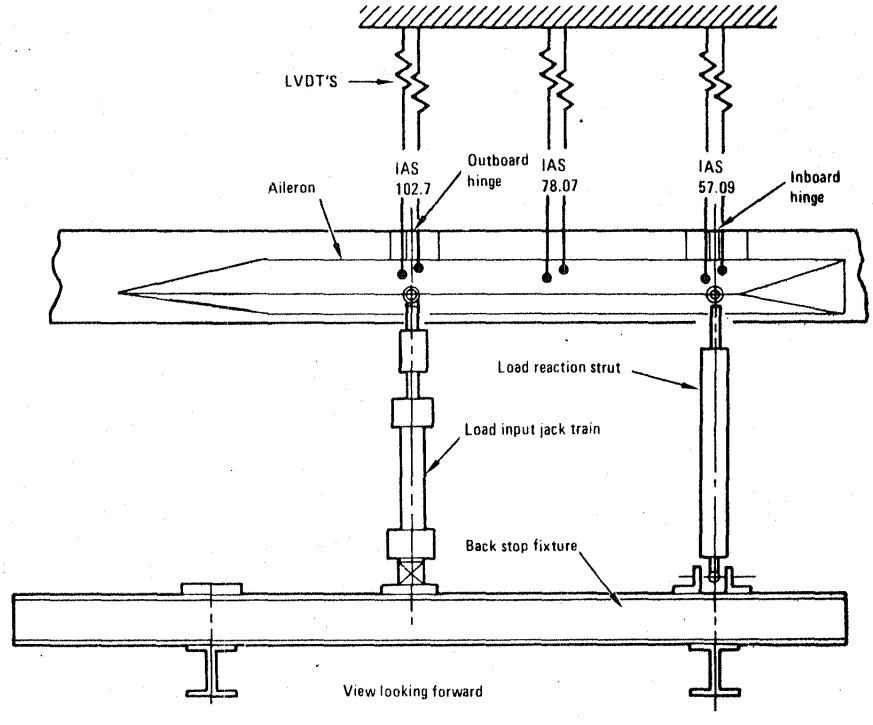


Figure 6. - Torsional stiffness test setup.

The values of required, predicted, and measured torsional stiffness for the metal aileron and two composite ailerons are presented in table 2. Note that the composite ailerons had slightly less stiffness than the metal aileron; however, their measured stiffness exceeded the structural requirements.

## 2.2 Vibration Tests

Vibration tests were conducted on the metal aileron and the first composite ground test article. These tests were conducted to determine the first flapping mode for one to three actuator links effective (see table 3) and for the Inboard Aileron Station (I.A.S.) 102.7 actuator link installed to stabilize the test article. The modal amplitude response was normalized to 10 g's at the intersection of the outboard closing rib and the rear spar and was maintained for all tests. A roving accelerometer was used on the lower aileron cover at several locations to monitor response. A photograph of the test set-up is shown on figure 7.

The vibration test results are presented in table 3. Note that several actuator conditions were investigated to evaluate the effect of various hydraulic system failures on frequency relationships.

TABLE 2. - TORSIONAL STIFFNESS COMPARISONS

| Torsional Stiffness $10^3$N-m$^2$ ($10^6$ lb-in$^2$) | Metal | Composite #1 | Composite #2 |
|---|---|---|---|
| Required | 861 (300) | 861 (300) | 861 (300) |
| Predicted | 1068 (372) | 1059 (369) | 1059 (369) |
| Measured | 1105 (385) | 961 (335) | 1079 (376) |

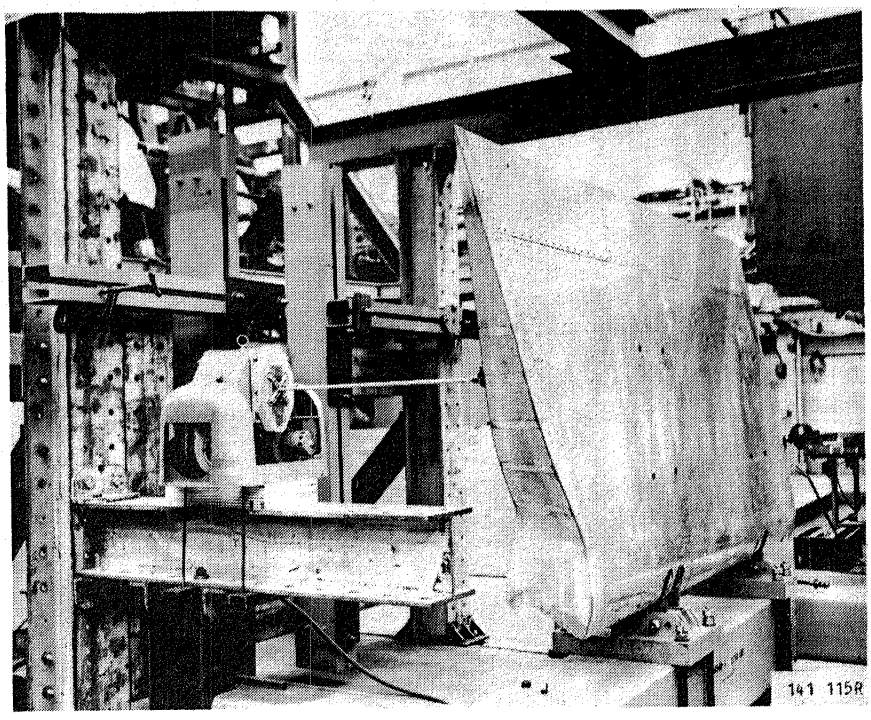


Figure 7. - Vibration test set-up.

TABLE 3. - FREQUENCY COMPARISONS

| Mode Type | Actuator Condition | Frequency - Hz | |
|---|---|---|---|
| | | Metal | Composite |
| Flapping | All Installed | 33.6 | 39.5 |
| Flapping | I.A.S.① 107.1 and 102.7 Installed | 28.4 | 29.6 |
| Flapping | I.A.S.① 102.7 Installed | 25.8 | 27.5 |
| Torsion | I.A.S.① 102.7 Installed | 47.1 | 48.1 |

① I.A.S. = Inboard Aileron Station

# 3. STATIC TESTS

## 3.1 Test Set-Up and Instrumentation

The full scale aileron assembly was mounted to a load reaction fixture with the hinge/actuator fittings. The actuator load reactions were simulated with adjustable links enabling the aileron angular attitude to be changed to accommodate the two loading conditions.

Pressure loads were applied to the upper surface of the aileron by pressure pads which were bonded to the surface with Goodrich 1273 adhesive at all rib and spar locations. Four hydraulic jacks in conjunction with a whiffle tree system were used to correctly distribute the applied loads. The loading system shown in figure 8 was designed to allow application of both tension and compression loads. A photograph of the aileron mounted in the test fixture is shown on figure 9.

The strain state of major elements within the aileron was monitored with 27 strain rosettes or axial strain gages as shown on figures 10, 11, and 12. Deflections at the various locations were measured by transducers located as

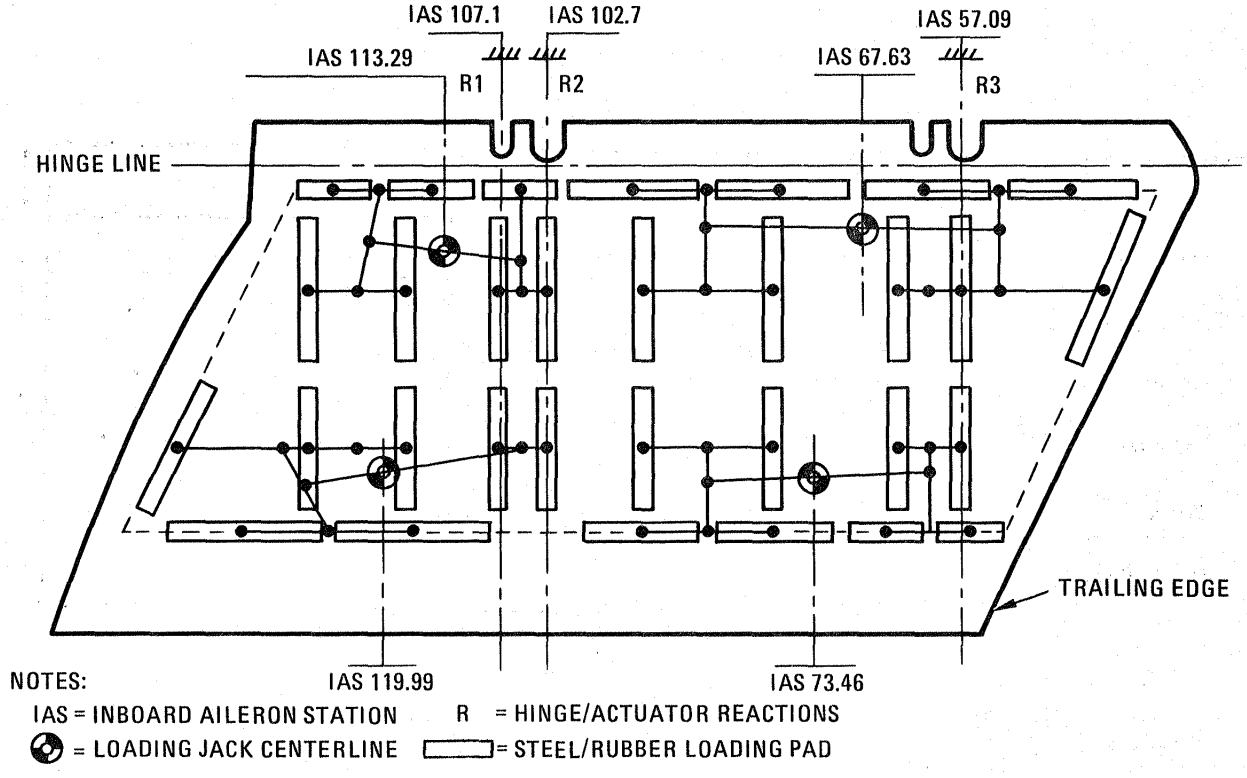


Figure 8. Loading Installation Arrangement Geometry

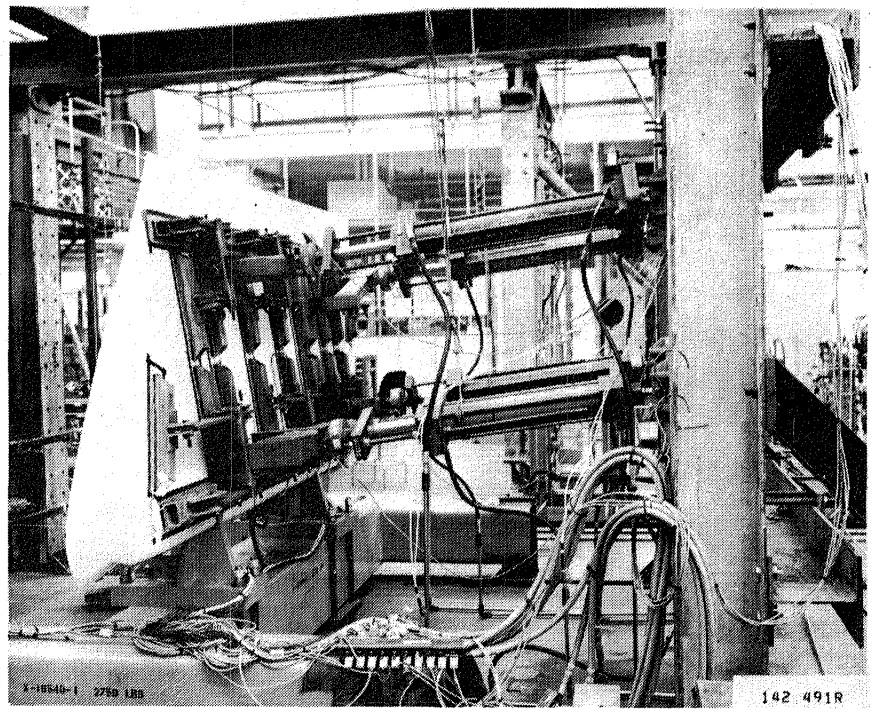


Figure 9. - Test set-up for static ground tests.

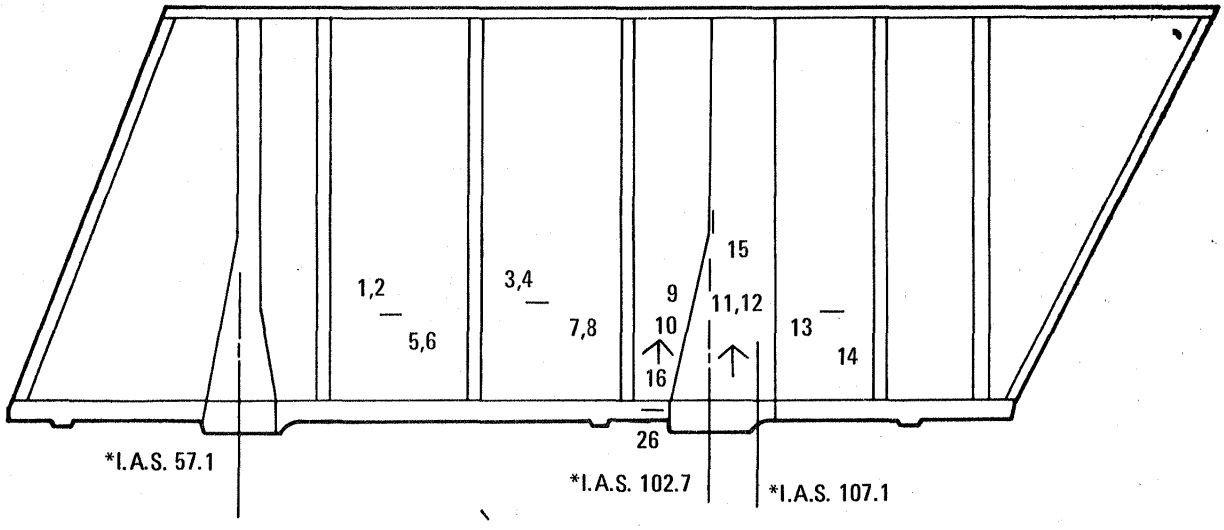


Figure 10. - Aileron cover (upper and lower) - strain gage locations.

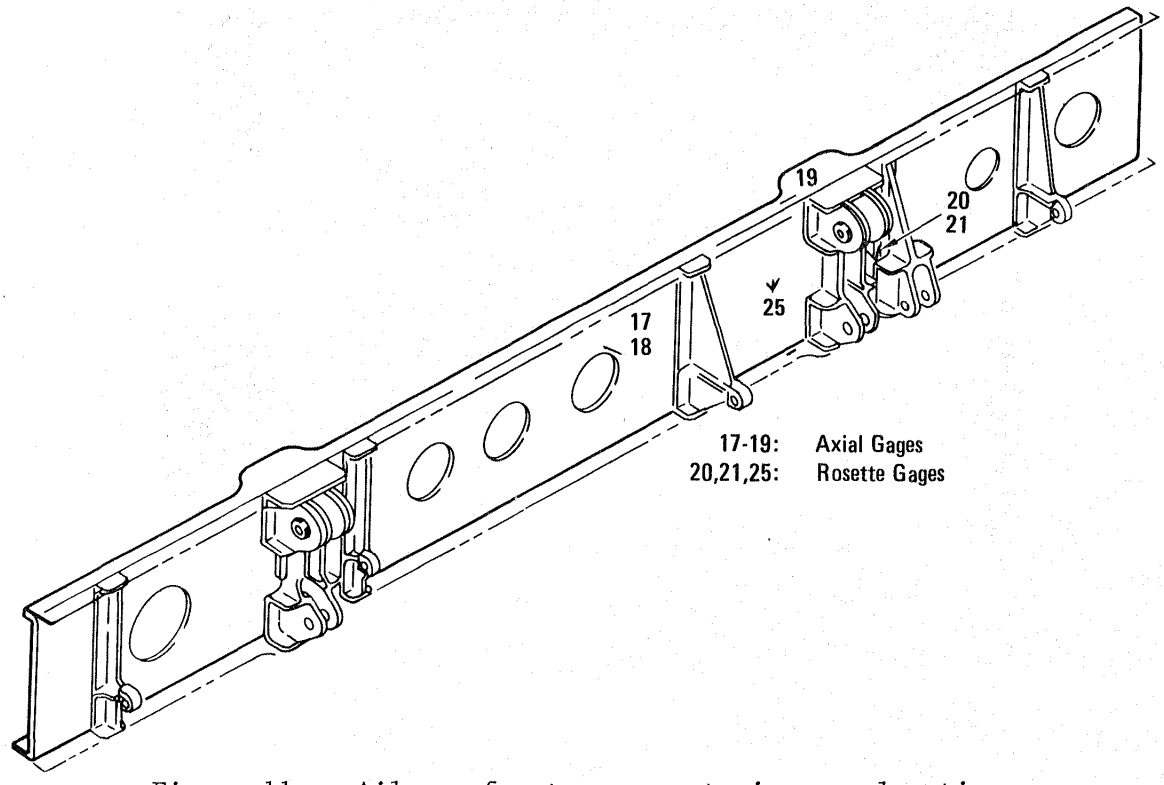


Figure 11. - Aileron front spar - strain gage locations.

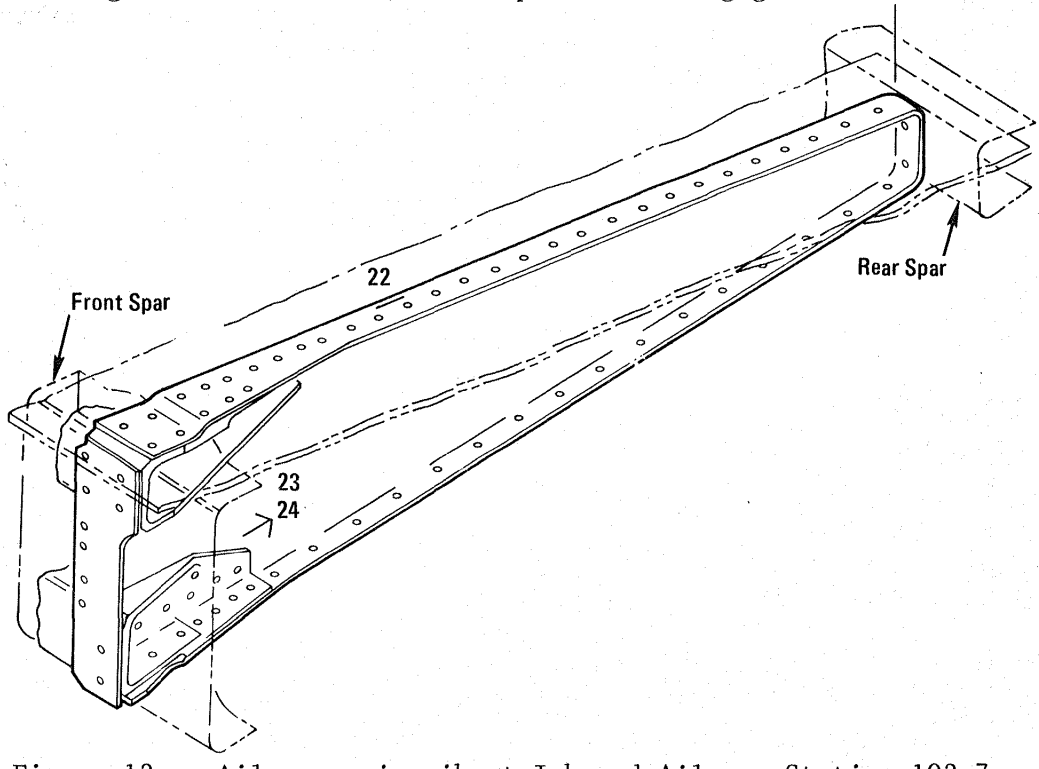


Figure 12. - Aileron main rib at Inboard Aileron Station 102.7 - strain gage locations.

shown on figure 13. Reactions to be the applied load were measured by strain gages applied to the adjustable links at the three actuator locations.

### 3.2 Test Conditions

Of the five basic design loading conditions on the aileron, the two most critical were simulated during the static tests of the composite aileron. These conditions are Condition 4, representing the $12^{o}$ down aileron deflection, and Condition 1, representing the $20^{o}$ up aileron deflection. These conditions stressed all the major elements of the aileron.

A structural analysis of the composite aileron was conducted to predict the failure loads, modes, and locations for the five design loading conditons. These predictions, shown in table 4, indicated that the lowest failure load for the aileron was 167 percent of design ultimate load for the Condition 3, 0 degree aileron deflection, loading. For this loading the predicted mode of failure was shear failure of the fasteners attaching the hinge/actuator fitting to the lower cover of the aileron. None of the composite parts of the aileron were critical for the Condition 3 loading. To minimize the number of loading conditions to be applied to the ground test article it was decided to increase the applied loads for Condition 4 to assure that the fasteners attaching the hinge/actuator fittings to the lower cover were loaded to design ultimate loads for Condition 3, thus 124 percent of the Condition 4 loads were applied to the aileron.

Environmental factors which affect the strength of various laminates on the composite aileron were determined by coupon tests at the environmental extremes. This data lead to the selection of an environmental factor of 1.17 to be multiplied times the design ultimate load. Thus the test requirement for the Condition 1 loading was 117 percent of design ultimate load when tested at ambient conditions.

### 3.3 Condition 4 Testing

The Condition 4 loading was applied to 67 percent of design ultimate load (DUL), and then to 124 percent DUL. Following the application of limit load and 124 percent DUL, there was no visible evidence of permanent deformation or damage.

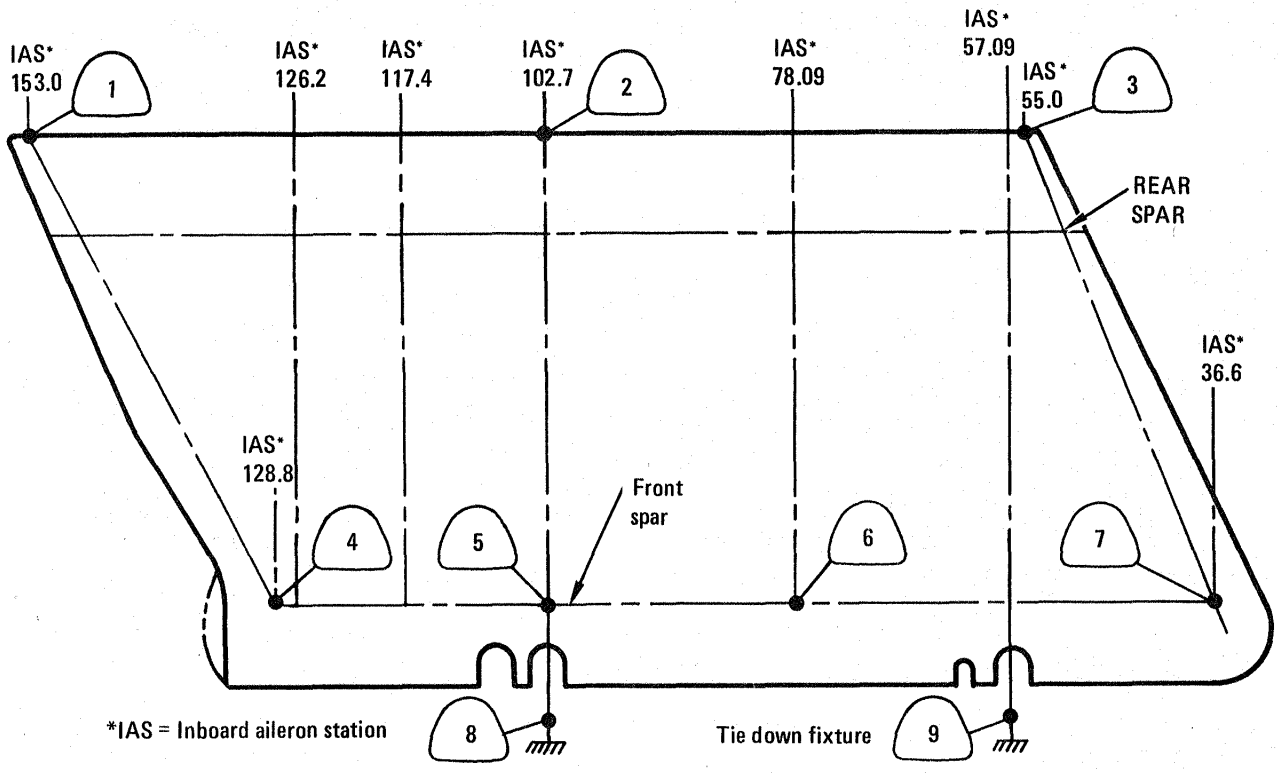


Figure 13. - Composite aileron deflection transducer locations.

TABLE 4. - PREDICTED AILERON FAILURE LOADS

| Predicted Failure Load at RTD (% DUL) | Location | Condition | Failure Mode |
|---|---|---|---|
| 167 | H/A Fitting Lower Fasteners | 3 | Fastener Shear |
| 171 | H/A Fitting Upper Fasteners | 2 | Fastener Tension |
| 181 ⚠1 ⚠2 | Spar Web @ IAS105 | 1 | Combined Shear |
| 183 | H/A Fitting Upper Fasteners | 1 | Fastener Tension |
| 200 ⚠2 | Lower Cover Attach to Front Spar | 1 | Bearing |
| 202 | H/A Fitting Lower Fasteners | 5 | Fastener Shear |
| 207 | H/A Fitting Lower Fasteners | 4 | Fastener Shear |
| 220 ⚠2 | Lower Cover Attach to Front Spar | 4 | Bearing |

⚠1 Based on the maximum load in the front spar test.

⚠2 These predictions are based on average strength design data.

H/A = Hinge/Actuator IAS = Inboard Aileron Station

The actuator link reactions are shown on figure 14. The hydraulic actuators give equal loads at the three stations by pressure-equalization, however this was not possible with solid links. It was necessary to apply a preload to the solid links to enable the link loads to be approximately equal at limit load. The link loads were within 9 percent of target. At 124 percent DUL the link load at IAS 102.7 was 103 percent of target, while at IAS 107.1 it was 82 percent of target.

Analysis indicated that for the Condition 4 loading the upper cover would buckle in compression at 24 percent of DUL. This behavior is illustrated on figure 15 which displays the spanwise strains in the inner and outer surface of the cover at I.A.S. 85.7. Buckling occurred at approximately 70 percent of DUL.

Aside from the upper cover, which was expected to buckle in compression in the spanwise direction, the majority of aileron deflections and element load-strain responses indicated a linear behavior of 100 percent of DUL.

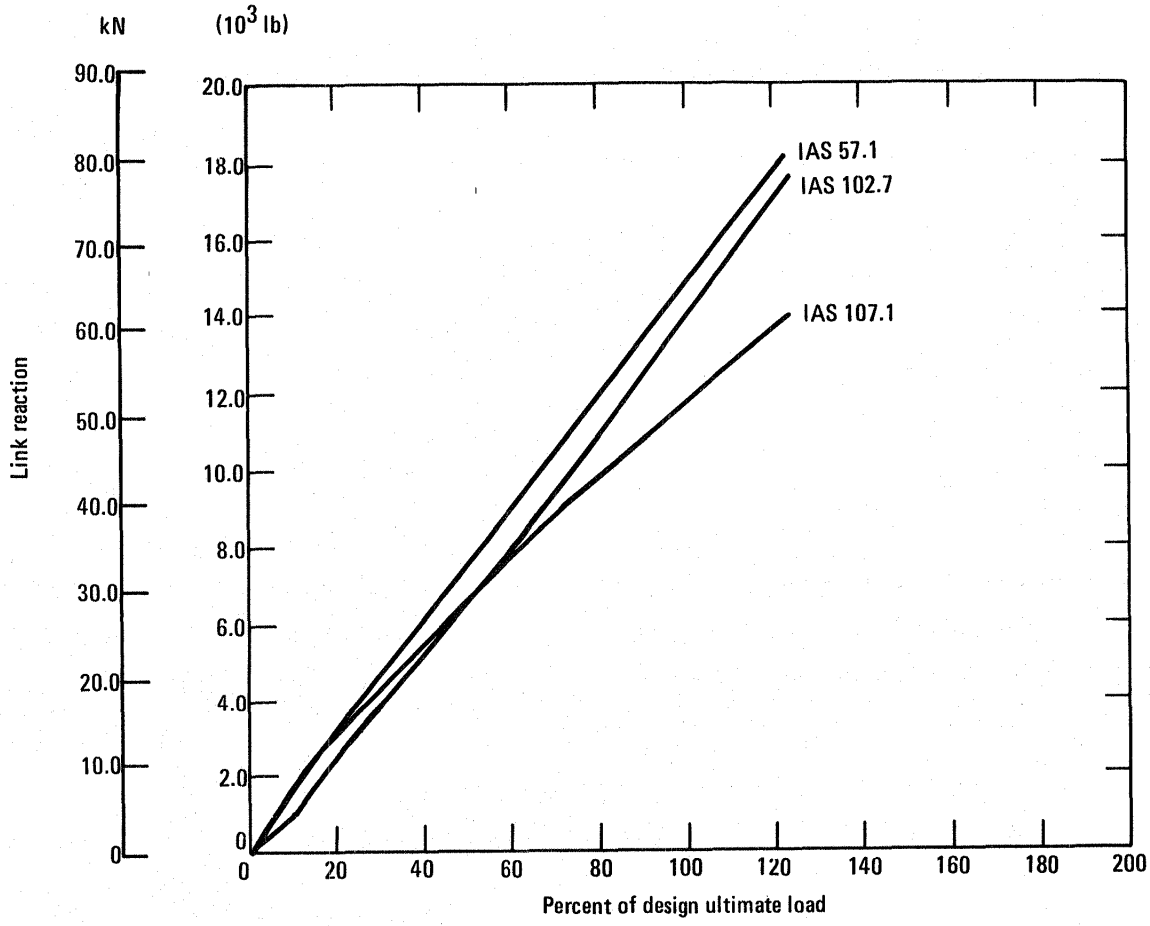


Figure 14. - Condition 4 actuator link reaction loads.

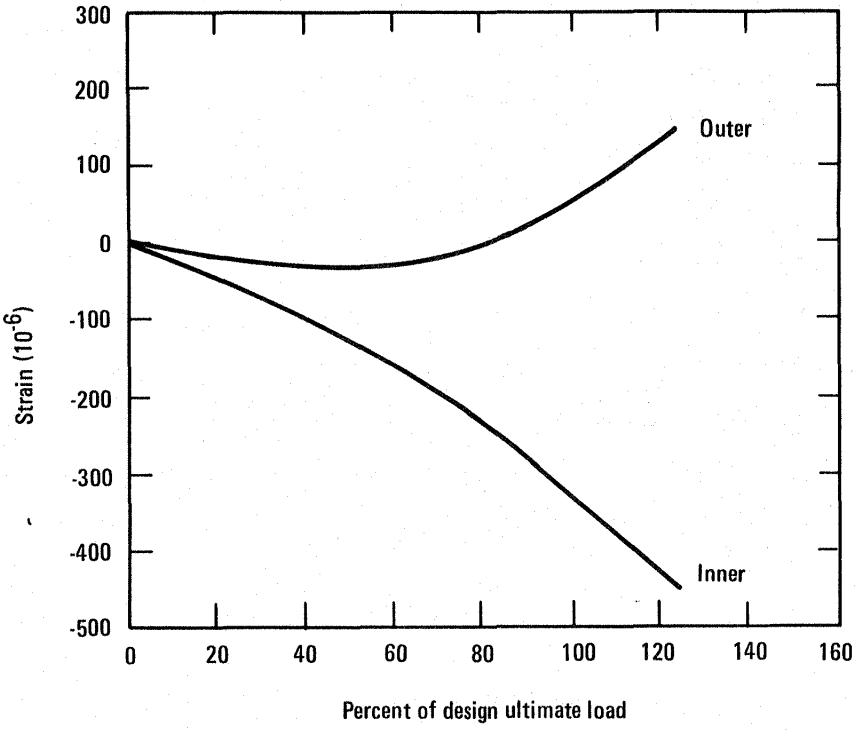


Figure 15. - Condition 4, upper cover strains at I.A.S. 85.7.

Linearity is illustrated by inspecting the cover/rib cap chordwise strain behavior at the hinge/actuator rib (figure 16) and the front spar cap (figure 17).

The back-to-back strain rosette data for the hinge/actuator rib web at I.A.S. 102.7 are shown on figures 18 and 19. These rosettes, located 218.4 mm (8.6 in) aft of the front spar web, indicate the initiation of rib web buckling at 90 percent of DUL.

### 3.4 Condition 1 Testing

Condition 1, $20^{o}$ up aileron position, loading was applied to 67 percent DUL and then to 117 percent DUL. Following the application of these loads the load-strain data were reviewed and there was no evidence of permanent deformation or damage to the aileron. As discussed earlier the additional 17 percent over DUL is an environmental factor.

Following these tests the aileron was loaded to failure in the Condition 1 configuration. Failure occurred at 139 percent DUL. The lower cover was removed (figure 19) to permit examination of the failed members. Neither the covers nor the front spar experienced visible damage. The station 102.7

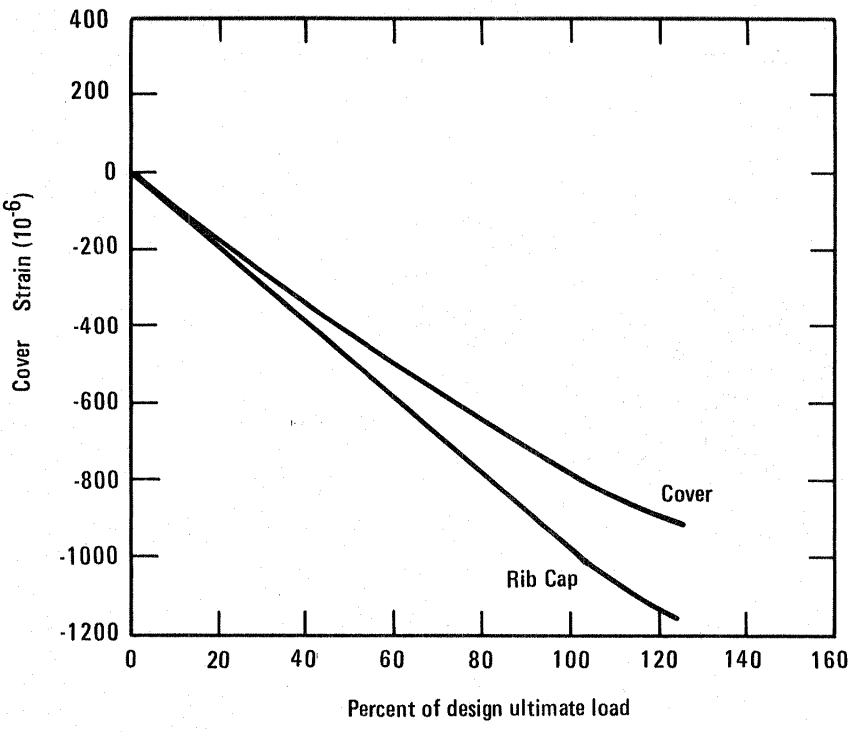


Figure 16. - Condition 4, chordwise strains-cover/upper rib cap at I.A.S. 102.7.

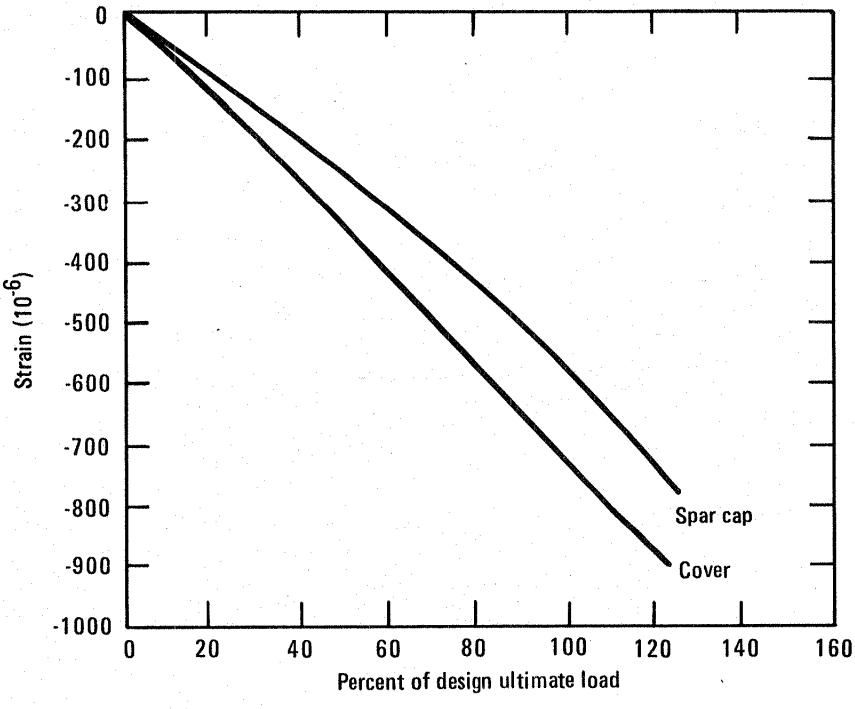


Figure 17. - Condition 4, spar cap strains at I.A.S. 97.4.

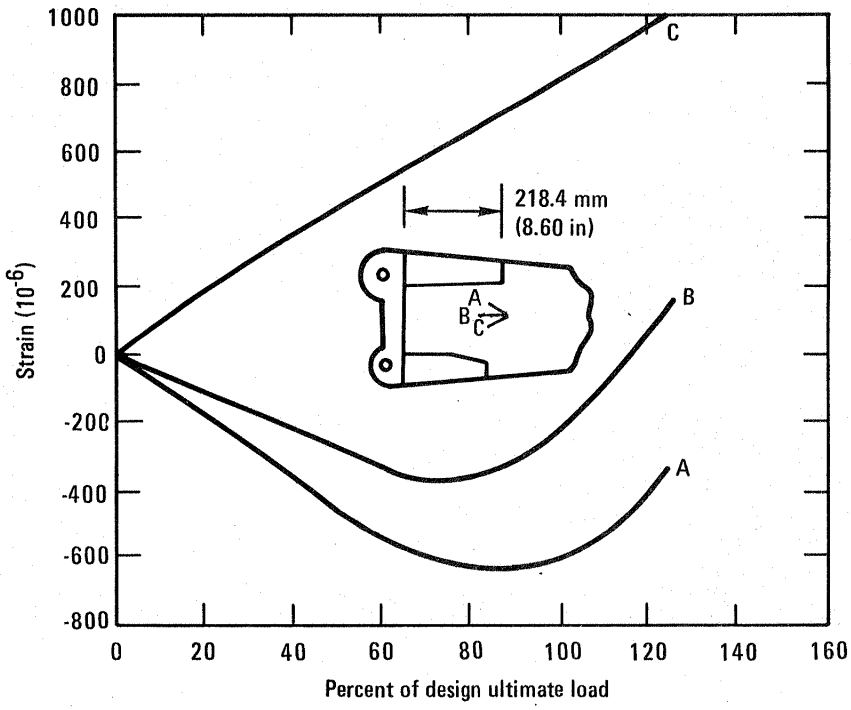


Figure 18. - Condition 4, I.A.S. 102.7 rib web strains at gage 23.

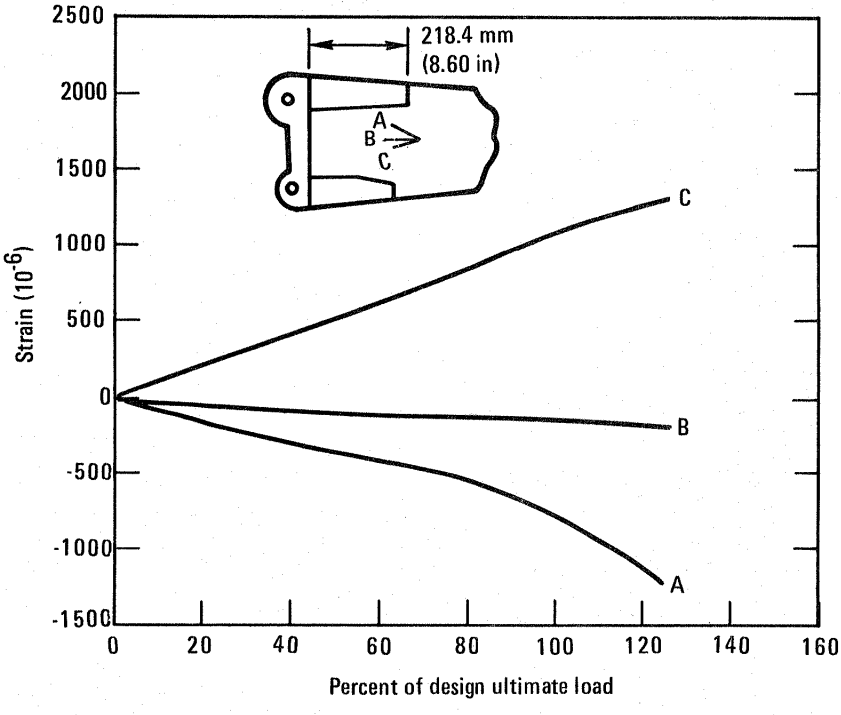


Figure 19. - Condition 4, I.A.S. 102.7 rib web strains at gage 24.

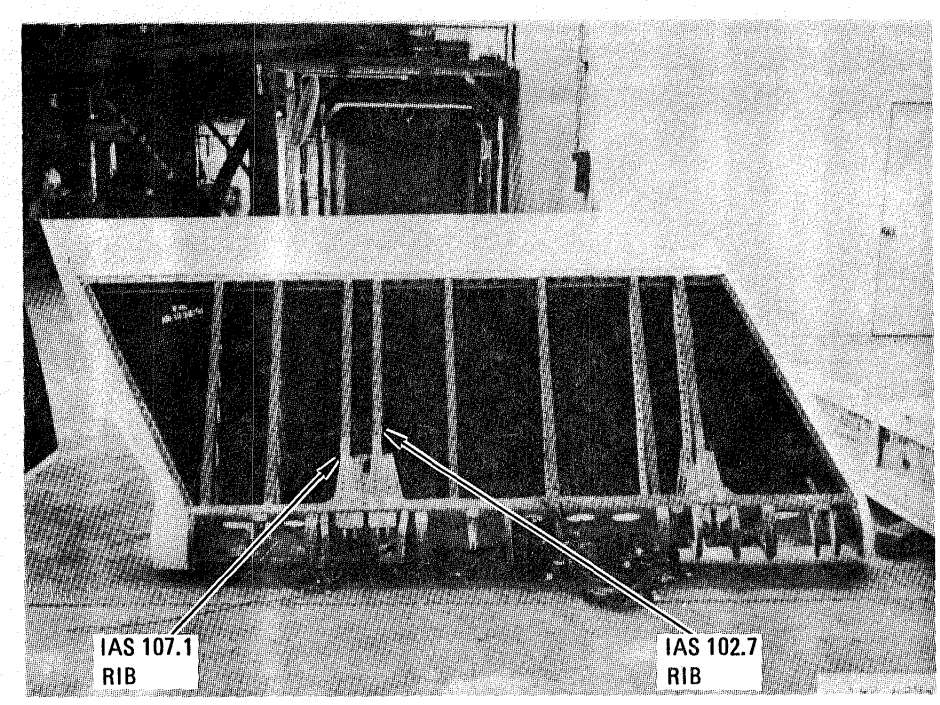


Figure 20. - Static ground test article with lower cover removed.

main rib web failed in a post-buckling mode with the web tearing at the bathtub fitting near the front spar and failing in bending along the crest of the shear buckle (see figures 21 and 22). The main rib web at station 107.1 also failed in buckling with the bending failure crossing the two forward access holes (figures 23 and 24). It is not possible to distinguish the sequence of failure of these two ribs because the measured actuator link loads at I.A.S. 102.7 and I.A.S. 107.1 show a load drop-off at exactly the same instant.

The load-strain response of the various elements within the aileron were similar to the Condition 4 load response in that most of the behavior was linear to 100 percent of DUL. As expected the lower cover buckled in compression in the spanwise direction. Analyses of the back-to-back rosettes on the hinge/actuator rib at I.A.S. 102.7 indicated initial buckling of the rib web at approximately 95 percent of DUL. The failure mode of the rib web appears to be a tensile failure precipitated by shear buckling of the web.

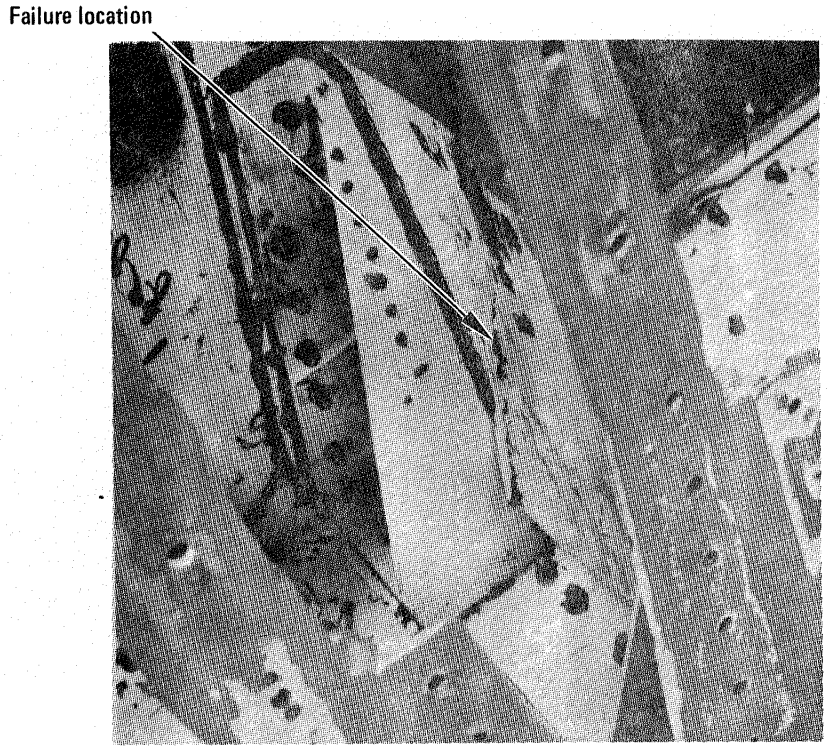


Figure 21. - Closeup view of I.A.S. 102.7 rib showing Web failure-outboard side.

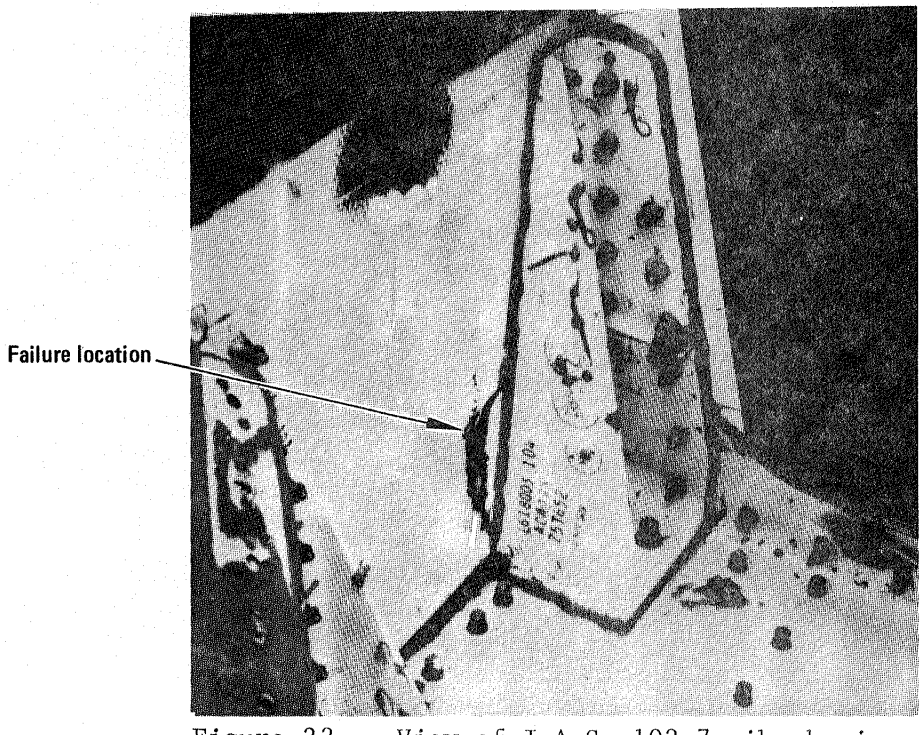


Figure 22. - View of I.A.S. 102.7 rib showing Web failure-inboard side.

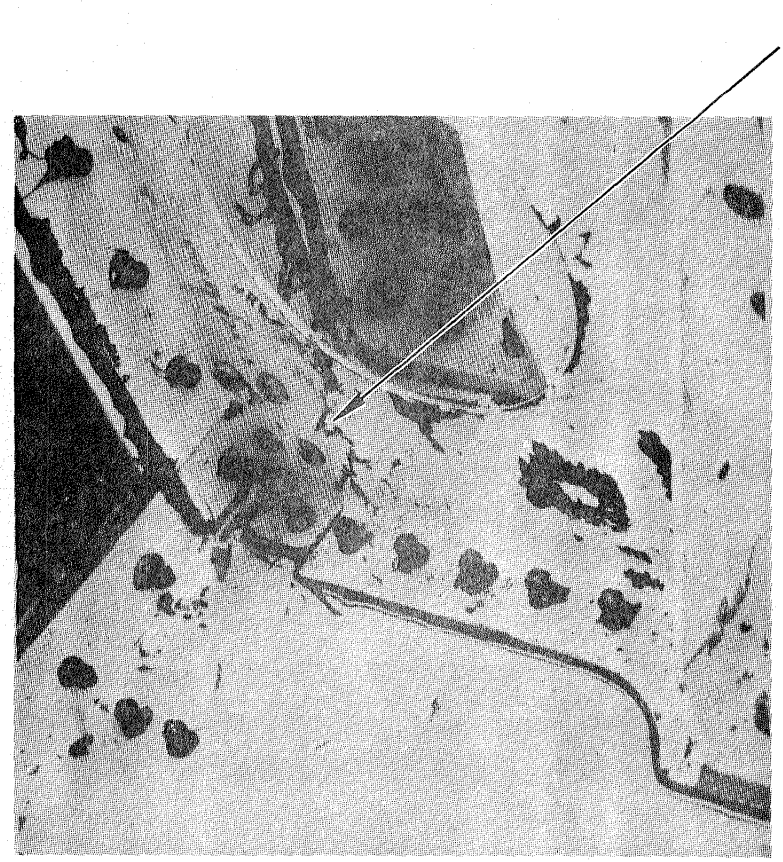


Figure 23. - Closeup view of I.A.S. 107.1 rib showing Web failure-outboard side.

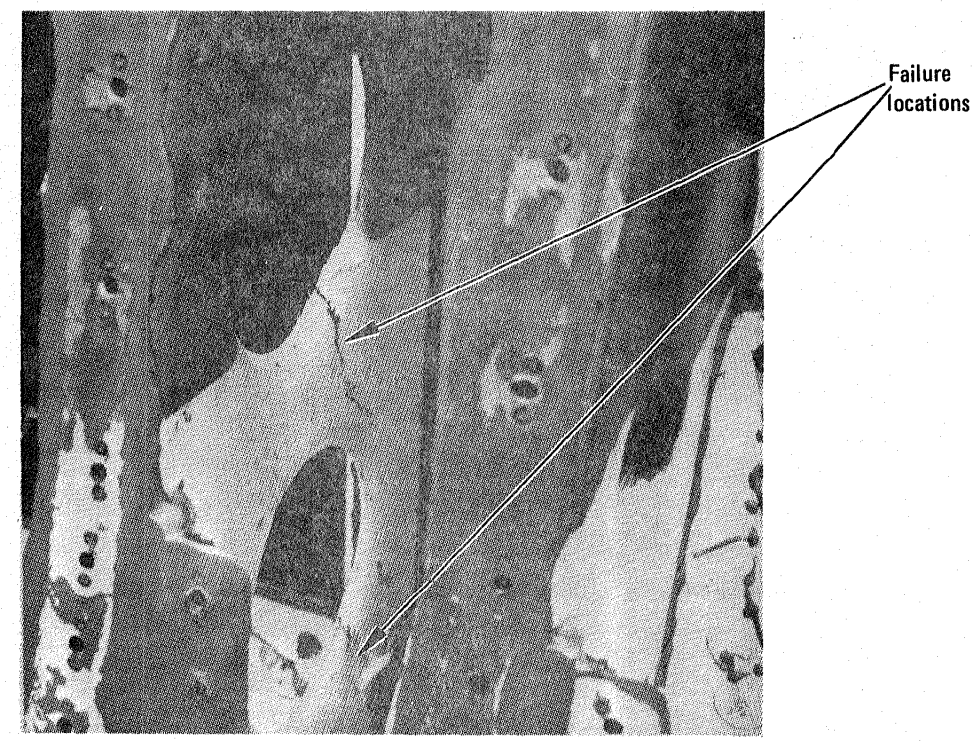


Figure 24. - View of I.A.S. 107.1 rib showing Web failure-inboard side.

The structural analysis of the rib webs at I.A.S. 102.7 and 107.1 had predicted buckling would occur at loads much greater than ultimate. This analysis was based on data from a three-dimensional finite element model in which the elements of the rib models were relatively large and thus the internal loads were dissipated over longer paths.

After completion of the static tests on the composite ground test article the hinge/actuator rib was reanalyzed using a two-dimensional finite element model which had a very fine grid. The purpose of this analysis was twofold: 1) to verify that the loads applied to the rib during the test accurately represented in flight loading condition, and 2) to provide verification that a more accurate analysis of the rib could predict failure.

As illustrated on figures 25 and 26 the results of the rib analysis show that the rib loads applied in the test were equivalent to those applied by the flight loading condition. Based on this analysis the predicted failure load for the rib web (using room temperature, dry average material properties) was 126 percent of design ultimate load.

The environmental factor of 117 percent used for the static test of the aileron was based on test data for the front spar web since this element had been predicted to fail first. Since the static test data from the aileron and a more detailed analysis of the hinge/actuator rib indicated that the rib web is the weakest element within the aileron a review of the environmental factors was conducted. Coupon test data on laminates representative of the rib web material indicated an environmental factor of 1.12 for tension loads and 1.06 for shear instability were required to account for environmental effects. Thus the 1.17 factor used for the static ground tests was more than adequate.

## 4. DAMAGE TOLERANCE/FAIL-SAFE TESTS

### 4.1 Test Set-Up and Instrumentation

The test fixtures, method of load application, and instrumentation utilized for the damage tolerance/fail-safe ground test article were the same as those used for the static ground test article.

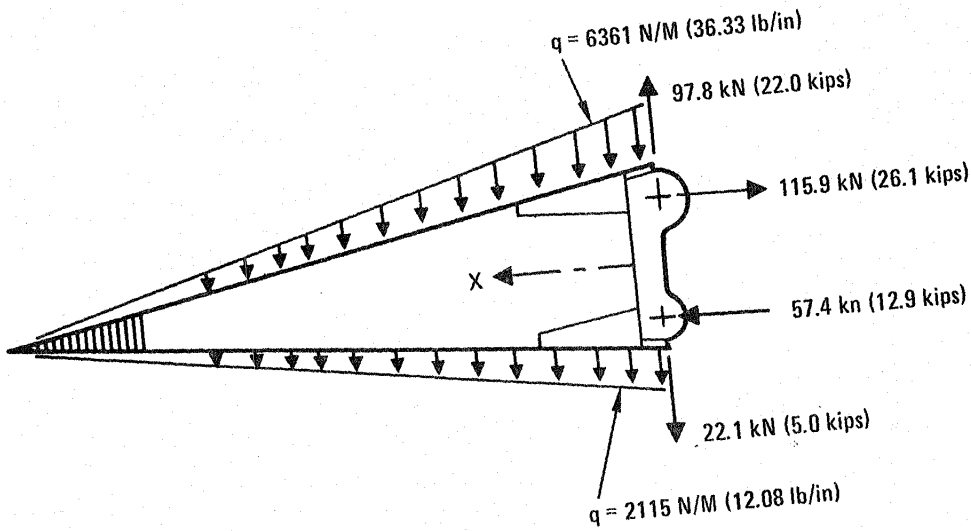


a) Condition 1 ultimate design loads

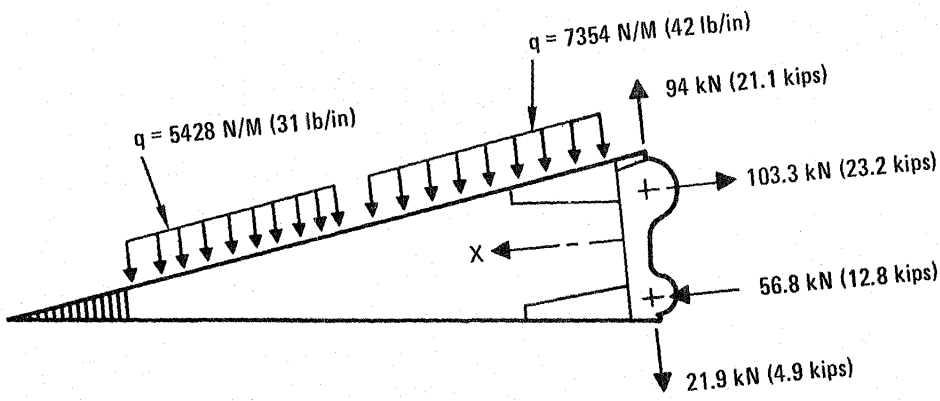


b) Condition 1 ultimate test loads

Figure 25. - Comparison of design loads to test loads for I.A.S. 102.7 rib.

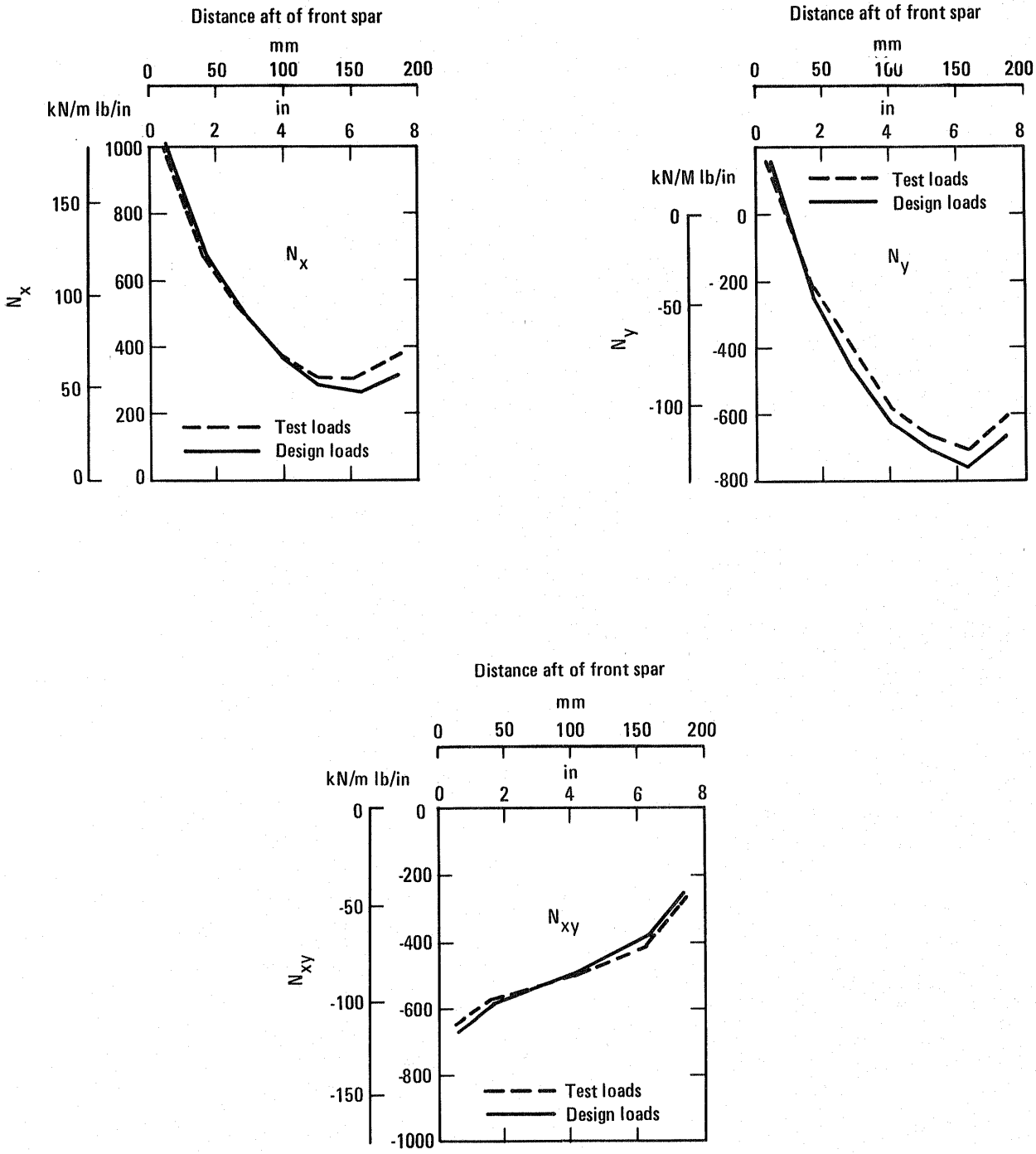


Figure 26. - Comparison of stress resultants - test loads versus design loads.

## 4.2 Damage Tolerance Tests

The objective of the damage tolerance tests was to verify that minor damage to the structure would not grow to a sufficiently large size due to flight loading between inspections to render the structure incapable of carrying limit load. The damage was of sufficient size to be visually detectable during a major inspection. One lifetime of spectrum fatigue loading was applied to the structure to determine damage growth characteristics. This is approximately twice the interval for major inspections.

Four locations on the aileron were selected for inflicting damage, the upper cover, the main rib cap, the front spar web, and the forward spar cap flange of the lower cover. The upper cover was impacted with 13.6 Joules (10 ft-lb) of energy. A 25.4 mm (1.0 in) diameter hemispherical steel impactor was used. The impact location was in the midst of the buckling region, at I.A.S. 85.7, 178 mm (7 in) aft of the front spar datum. The upper cap of the I.A.S. 102.7 rib was cut prior to assembly. The cut extended from the edge of the fastener hole, located 244 mm (9.6 in) aft of the front spar datum, through the cap thickness to the free edge of the cap. With the impactor described above, the front spar web was impacted with 8.1 Joules (6 ft-lb) of energy. The impact location was I.A.S. 105.0, approximately 89 mm (3.5 in) above the lower cap. The forward flange of the lower cover was impacted with 13.6 Joules (10 ft-lb) of energy. This region acts as part of the front spar cap. The impact location was I.A.S. 99.0, approximately 12.7 mm (.5 in) aft of the free edge. All of these impacts caused visible damage on both the front and back surfaces of the component. Nondestructive inspections were made to quantify the amount of damage. A photograph of the damage to the upper cover is shown on figure 27.

The L-1011 flight-by-flight fatigue loading spectrum was applied for one lifetime of 36,000 flights. This represents 67,000 flight hours. Damage growth inspections, both visual and ultrasonic, were conducted after one-half lifetime of load application and upon completion of the test. No growth was found at the one-half lifetime interval. After completion of one lifetime only one of the four damaged areas had grown, this was the

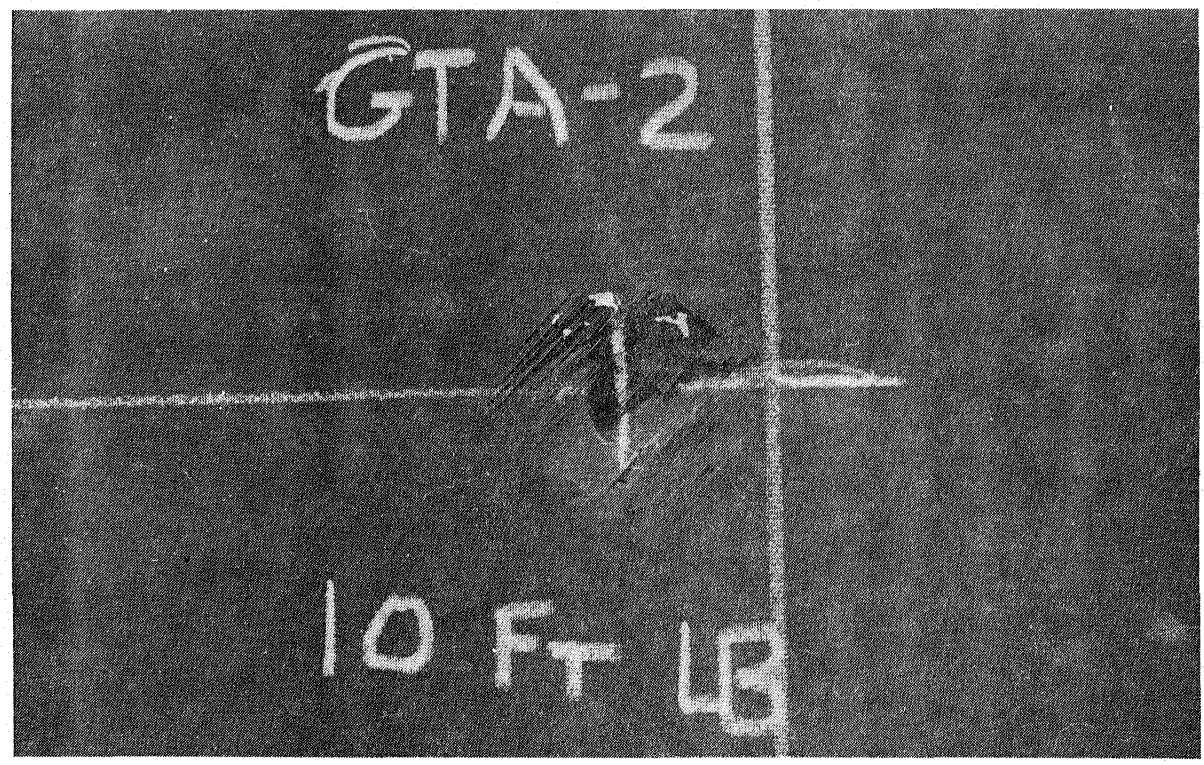


Figure 27. - Upper cover impact damage.

impact damage on the upper cover. The damage had increased in size from a 51 mm (2.0 in) diameter circle to an ellipse with a major axis dimension of 152 mm (6.0 in). Subsequently, 117 percent of limit load for Condition 1 and 117 percent of limit load for Condition 4 were applied to demonstrate that this damage had not grown to critical size. The load/strain data taken during these tests were not significantly different from those obtained from similar tests applied to the undamaged ground test article. The exceptions include the gage near the cut rib cap at I.A.S. 102.7, where the axial strains were 20 percent less; and the back-to-back rosettes on the front spar web at I.A.S. 105 near the impact damage, where the shear strains were 10 percent less.

The application of these loads (which include a 17 percent environmental factor) demonstrated that the aileron can sustain substantial damage any time during the period between major inspections without compromising its structural integrity.

## 4.3 Fail-Safe Tests

The composite aileron was designed to be a fail-safe structure. Fail-safe tests were conducted on the aileron to verify that the structure would be able to withstand static loads which are reasonably expected during the completion of the flight in which damage resulting from obvious discrete sources occurs. An assessment was made of service mission and potential damage relating to each discrete source. This assessment included lightning strike tests and hailstone impacts on full scale sections of the composite aileron. It was determined that the damage from swept-stroke lightning was the most detrimental discrete source damage.

The area selected for the damage was the lower cover at I.A.S. 85.7, 191 mm (7.5 in) aft of the front spar. To simulate the damage from swept-stroke lightning the following procedure was utilized. The cover was subjected to five impacts of 10.8 J (8 ft-lb) of energy each along a $45^{o}$ line spaced approximately 51 mm (2 in) apart. A 25.4 mm (1.0 in) diameter steel rod with a hemispherical tip was used to make these impacts. Ultrasonic inspection of the cover after the impacts (shown in figure 28) verified that substantial delamination occurred over a region of 381 mm (15 in) by 76 mm (3 in). A welder's electric arc was then used to burn a hole in the middle of the delaminated area, see figure 29. An oxygen/acetelene torch was then used to burn the surface of the entire delaminated area. The resulting damage, shown on figure 30, satisfactorily simulated the effects of swept stroke lightning.

After the discrete source damage was inflicted to the aileron, the fail-safe tests were conducted. The four previously damaged areas on the aileron were not repaired prior to the fail-safe or residual strength tests.

To satisfy Federal Aviation Administration (FAA) requirements, the ability to withstand static loads which could be reasonably expected during completion of a flight following the discrete source damage must be demonstrated. A load equal to 70 percent of design limit load complies with this requirement. Because the test was conducted under ambient conditions a 17 percent environmental factor was included, bringing the test load to 82 percent of limit load.

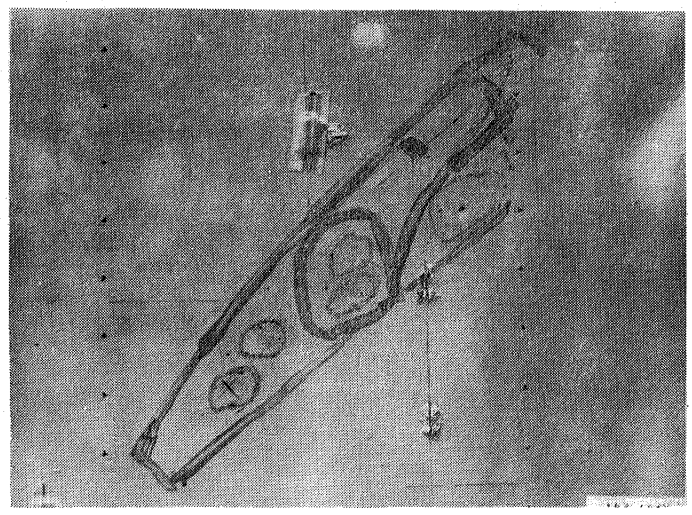

Figure 28. - Lower surface impact delamination (front face).

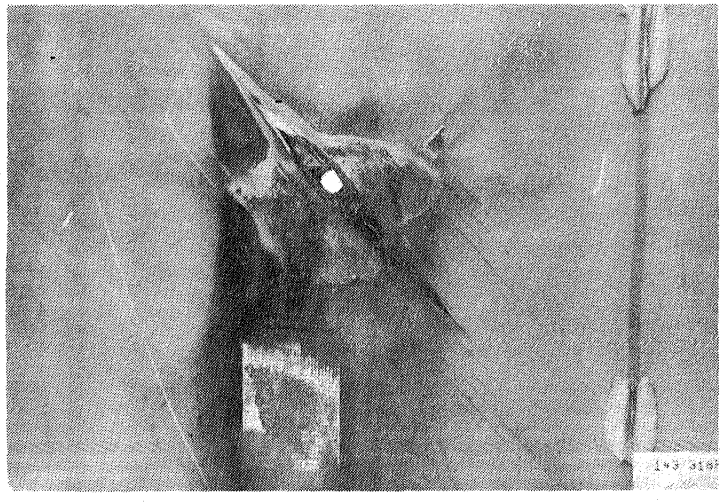

Figure 29. - Lower surface burn-through and impact damage (back face).

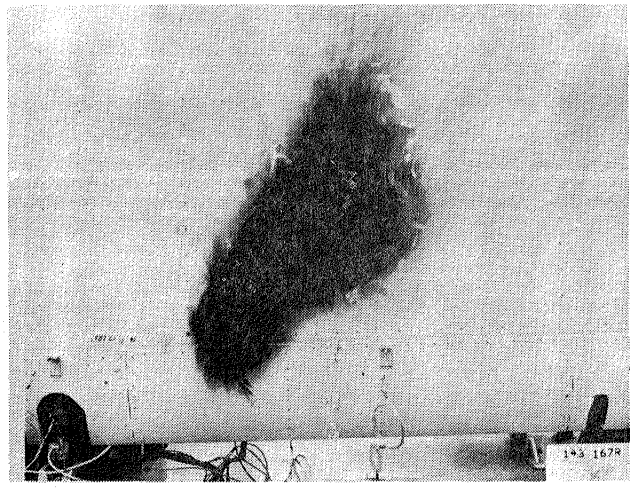

Figure 30. - Lower surface swept-stroke damage simulation.

The damaged aileron was successfully loaded to 82 percent of limit load for both Condition 4 and Condition 1. The actuator load links were positioned to the correct angle and adjusted to give nearly equal link loads at the maximum test load for each condition. For both of these loading conditions there was neither failure nor visible evidence of damage growth. The load/strain data taken during these tests were not significantly different than those at the same load level taken during the damage tolerance tests. One of the exceptions included the back-to-back axial gages on the lower cover at I.A.S. 85.7 near the lightning damage which showed buckling occurred at 63 percent of limit load as compared to buckling at 76 percent of limit load before the lightning damage. The other exception was the axial gage at the leading edge of the lower cover at I.A.S. 95. Its trace flattened out above 50 percent of limit load, possibly indicating some local buckling.

### 4.4 Residual Strength Test

Following all of these tests the aileron was loaded to failure in the Condition 1 configuration to determine its residual static strength. Failure occurred at 130 percent of design ultimate load in the postbuckling rupture of the rib webs at stations 102.7 and 107.1, shown on figures 31 and 32. The failure mode was the same as occurred for the static test article, but the failure load was 93.5 percent of the failure load for the undamaged test article. Other than the effect of internal load redistribution there was no evidence that any of the damage sites directly contributed to the failure. Following the initial failure at 130 percent of design ultimate load the load jacks continued to apply another 9 percent of design ultimate load before the load was dumped. This overload led to the failure of the station 57.1 rib web, followed by a failure of the covers and hinge fitting forging.

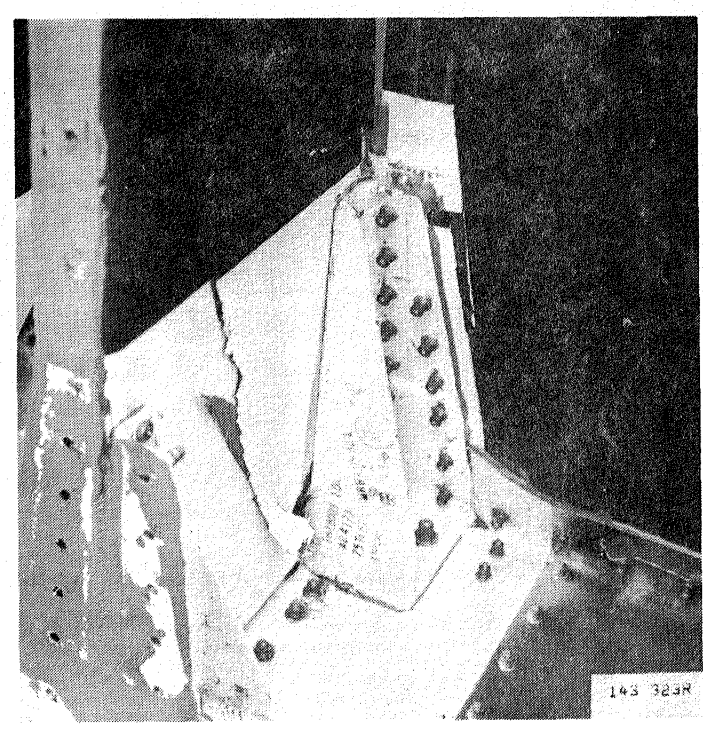

Figure 31. - I.A.S. 102.7 rib web failure, residual strength test.

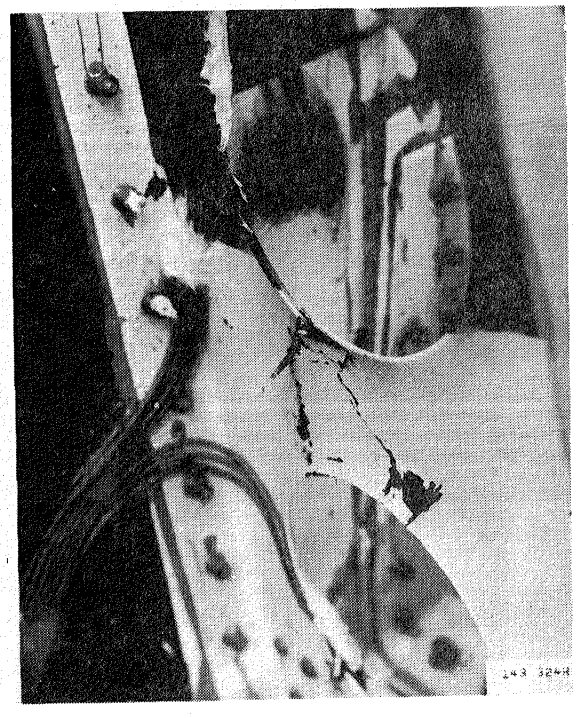

Figure 32. - I.A.S. 107.1 rib web failure, residual strength test.

## 6. FLIGHT CHECK-OUT

The flight of the advanced composite inboard ailerons was successfully completed in June of 1980. The first shipset of inboard composite ailerons was installed on the Lockheed L-1011 flight test aircraft. The aircraft take-off gross weight (TOGW) was 160000 kg (353,000 lb). The ailerons were ballasted with lead tape to achieve a worst-case hinge unbalance of 226 N-m (2000 in-lb). Ground servo stability during engine run up, level flight, and high-speed descent tests were performed as shown on figure 33. During these tests one or two of the three hydraulic servos were shut off to simulate fail-safe system conditions. Pulses were applied to the control column to give a momentary longitudinal pitch or lateral right or left roll impulses.

The advanced composite aileron response was somewhat better than the metal aileron during ground engine run up, and the damping characteristics of the composite aileron were comparable to the metal aileron during all tests. The composite aileron was flutter-free throughout the flight envelope.

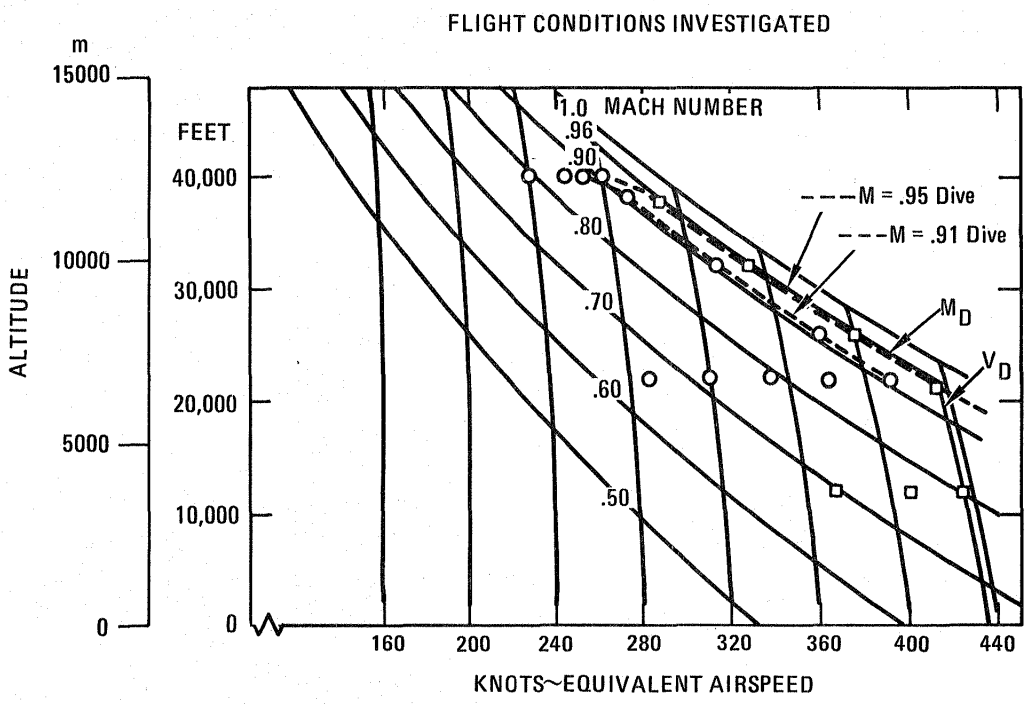


Figure 33. - Flight conditions investigated.

## CONCLUSIONS

Comparative stiffness and vibration tests were conducted on a metal aileron and two composite ailerons. These tests verified that the torsional stiffness of the composite aileron exceeded design requirements and that its vibration characteristics were similar to the metal aileron. The flight tests of the composite ailerons confirmed that the aileron was flutter-free throughout the flight envelope.

Static tests were conducted on a full scale composite aileron to verify structural integrity. In the upload condition, the aileron was statically loaded to 124 percent of design ultimate load without any damage or permanent deformation. On the download condition, the aileron was loaded to failure. Failure occurred at 139 percent of design ultimate load. These test results verified the static strength of the composite inboard aileron.

A second composite ground test article was subjected to damage growth/fail-safe tests. Visible damage was inflicted to the aileron in four locations. After the completion of one lifetime of spectrum fatigue loading little damage growth had occurred. Subsequent application of 117 percent of design limit load for two loading conditions demonstrated that the aileron can withstand substantial damage between inspection periods without compromising its structural integrity.

Fail-safe tests were then performed on the aileron with the four previously damaged areas and an additional large damage to the lower cover which simulated swept-stroke lightning damage. The structure was loaded to 82 percent of design limit load without any failures or permanent damage. The aileron was then loaded to failure to determine its residual strength. Failure occurred at 130 percent of design ultimate load in a failure mode identical to the undamaged aileron. The damage growth/fail-safe tests successfully verified the damage tolerance of the composite aileron design.

| 1 Report No | 2 Government Accession No | 3 Recipient's Catalog No |
|---|---|---|
| NASA-CR-165664 | | |

| 4 Title and Subtitle | 5 Report Date |
|---|---|
| Advanced Composite Aileron For L-1011 Transport Aircraft: Ground Tests and Flight Evaluation | February 1981 |
| | 6 Performing Organization Code D76-23 |

| 7 Author(s) | 8 Performing Organization Report No |
|---|---|
| C. F. Griffin | LR 29676 |
| | 10 Work Unit No |

| 9 Performing Organization Name and Address | 11 Contract or Grant No |
|---|---|
| LOCKHEED-CALIFORNIA COMPANY<br>P. O. BOX 551<br>BURBANK, CALIFORNIA 91520 | NAS 1-15069 |
| | 13 Type of Report and Period Covered January 1980 to December 1980 |

| 12 Sponsoring Agency Name and Address | 14 Sponsoring Agency Code |
|---|---|
| National Aeronautics and Space Administration<br>Washington, D. C. 20546 | |

15 Supplementary Notes
Langley Technical Monitor: Dr. Herbert A. Leybold
Final Report

16 Abstract
The activities documented in this report are associated with Task IV of the Advanced Composite Aileron program.

A composite aileron and a metal aileron were subjected to a series of comparative stiffness and vibration tests. These tests showed that the stiffness and vibration characteristics of the composite aileron are similar to the metal aileron.

The first composite ground test article was statically tested to failure which occurred at 139 percent of design ultimate load. The second composite ground test article was tested to verify damage tolerance and fail-safe characteristics. Visible damage was inflicted to the aileron and the aileron was subjected to one lifetime of spectrum fatigue loading. After conducting limit load tests on the aileron, major damage was inflicted to the cover and the aileron was loaded to failure which occurred at 130 percent of design ultimate load.

A shipset of composite ailerons were installed on Lockheed's L-1011 flight test aircraft and flown. The composite aileron was flutter-free throughout the flight envelope.

| 17 Key Words (Suggested by Author(s)) | 18 Distribution Statement |
|---|---|
| Composites, Materials, Secondary Structure Design, Testing, Transport Aircraft, Graphite Epoxy | FEDD Distribution |

| 19 Security Classif (of this report) | 20 Security Classif (of this page) | 21 No of Pages | 22 Price* |
|---|---|---|---|
| Unclassified | Unclassified | 34 | |



Available: NASA's Industrial Applications Centers

End of Document